AGU PUBLICATIONS

Geophysical Research Letters

RESEARCH LETTER
10.1002/2014GL059476

Key Points:
- We explore the general features of tremors in a collisional mountain belt
- Earthquake swarms correlate with the deep-seated tremors in time and space
- Metamorphic dehydration and fluid-pressure processes are the critical drivers

Supporting Information:
- Readme
- Figure S1
- Figure S2
- Figure S3
- Figure S4
- Figure S5
- Figure S6
- Figure S7

Correspondence to:
K. H. Chen,
katepili@gmail.com

Citation:
Chuang, L. Y., K. H. Chen, A. Wech, T. Byrne, and W. Peng (2014), Ambient tremors in a collisional orogenic belt, *Geophys. Res. Lett.*, *41*, 1485–1491, doi:10.1002/2014GL059476.

Received 31 JAN 2014
Accepted 3 FEB 2014
Accepted article online 6 FEB 2014
Published online 10 MAR 2014

Ambient tremors in a collisional orogenic belt

Lindsay Yuling Chuang[1], Kate Huihsuan Chen[1], Aaron Wech[2], Timothy Byrne[3], and Wei Peng[4]

[1]Department of Earth Sciences, National Taiwan Normal University, Taipei, Taiwan, [2]4210 University Dr., U.S. Geological Survey, Anchorage, Alaska, USA, [3]Geography Department, University of Connecticut, Storrs, Connecticut, USA, [4]Department of Geophysics, Tohoku University, Tohoku, Japan

Abstract Deep-seated tectonic tremors have been regarded as an observation tied to interconnected fluids at depth, which have been well documented in worldwide subduction zones and transform faults but not in a collisional mountain belt. In this study we explore the general features of collisional tremors in Taiwan and discuss the possible generation mechanism. In the 4 year data, we find 231 ambient tremor episodes with durations ranging from 5 to 30 min. In addition to a coseismic slip-induced stress change from nearby major earthquake, increased tremor rate is also highly correlated with the active, normal faulting earthquake swarms at the shallower depth. Both the tremor and earthquake swarm activities are confined in a small, area where the high attenuation, high thermal anomaly, the boundary between high and low resistivity, and localized veins on the surfaces distributed, suggesting the involvement of fluids from metamorphic dehydration within the orogen.

1. Introduction

As one of the youngest and most active collisional mountain belts, Taiwan is a natural laboratory for studying seismic behavior associated with orogen-wide fluid generation. This island is located at the complicated plate boundary zone between the Eurasian Plate (EP) and the Philippine Sea Plate (PSP). In northeast Taiwan, the PSP subducts northwest beneath the rifted Eurasian Plate margin along the Ryukyu Trench at a rate of 8 cm/yr [*Seno et al.*, 1993; *Yu et al.*, 1997], whereas in southwest Taiwan, the Eurasian Plate subducts beneath the PSP along the Malina Trench. The resulting collision between the eastward subducting Eurasian lithosphere and overriding Luzon volcanic arc [*Biq*, 1973; *Bowin et al.*, 1978; *Ho*, 1986] creates the Taiwan's Central Range. This active mountain belt (gray areas III–V in Figure 1) is a very young orogen characterized by rapid exhumation of metamorphic rocks exposed in the eastern Central Range [*Willett et al.*, 1993, 2003]. The southern Central Range, an area experiencing extremely rapid uplift (15–20 mm/yr) [*Ching et al.*, 2011], normal faulting earthquake activities [*Hsu et al.*, 2010], high heat flow [*Chi and Reed*, 2008; *Yamato et al.*, 2009], and low electrical resistivity [*Bertrand et al.*, 2012], has been regarded as a natural laboratory for studying the interactions of tectonic processes and fluid flow. However, direct measurement of seismic behavior from greater depth, which is important for understanding fluid flow and deformation at depth, has been lacking due to the paucity of seismicity below a depth of 25 km.

Deep, tectonic tremors recently discovered in worldwide subduction zones and fault systems open the door for studying deformation processes at greater depth. Noise-like, nonvolcanic tremors are found to play an important role in a broad spectrum of strain release processes, especially in the transition zone between stable sliding and locked portions of faults. Given that the duration of tremors scales with the magnitude of accompanying slow slip events [*Ide et al.*, 2007; *Aguiar et al.*, 2009], deep-seated tremors are regarded as an indicator for slow slip and are often interpreted as a result of shear slip assisted by high fluid pressures [e.g., *Shelly et al.*, 2006, 2007; *Wech and Creager*, 2007]. In the area where the slow slip events are too small to be detected geodetically, monitoring of tremor activity provides crucial information into the complex deformation below the base of seismogenic zone.

Tremor episodes in Taiwan triggered by distant $M > 7$ events (green circles in Figure 1) illustrate the generation potential of nonvolcanic tremors underneath the Central Range, where they have been inferred to occur on an east dipping basal detachment beneath the Central Range [*Peng and Chao*, 2008; *Tang et al.*, 2010], consistent with the simple one-sided wedge model for Taiwan orogen [e.g., *Suppe*, 1981; *Davis et al.*, 1983; *Carena et al.*, 2002]. Ambient tremors are also found in the same area and are characterized by relatively short durations from several to tens of minutes compared with subduction zone tremors. Short-duration targets, coupled with high

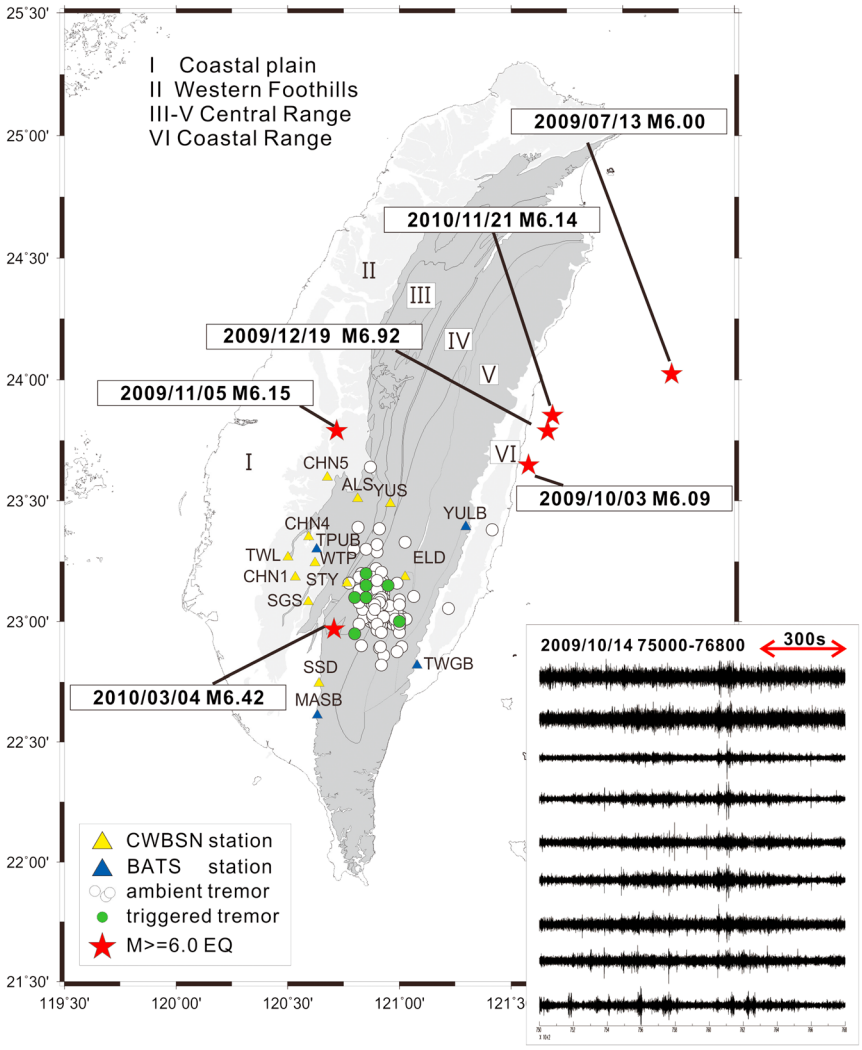

Figure 1. Local seismicity and tremor distribution. Red stars denote $M \geq 6.0$ earthquakes that occurred during the study period from 2008 to 2011. Green and white circles denote triggered tremor [*Chao et al.*, 2012] and ambient tremor, respectively. Yellow and blue triangles indicate Central Weather Bureau Seismic Network and Broadband Array in Taiwan for Seismology stations, respectively. The major tectonostratigraphic units are denoted by I to VI. Inset shows example of ambient tremor in a 30 min long seismogram recorded at nine stations (2–8 filtered, E-W component).

noise levels and sparse seismic network coverage, make automatic detection in this region challenging. In this study we develop an adaptive detection scheme to automatically identify ambient tremors in this region. We then, compare the tremor spatial and temporal activities with regional seismicity to infer possible generation mechanisms.

1.1. Detection of Ambient Tremors

Applying the envelope cross-correlation-based scheme (see supporting information for ambient tremor detection method) to 4 year data starting from January 2008 to December 2011, we detect 231 ambient tremor episodes with durations ranging from 5 to 30 min (waveform example shown in inset to Figure 1 and Figure S1 in the supporting information). Note that the tremors triggered by teleseismic events are excluded in our catalog. Among the 231 ambient tremors (white circles in Figure 1), 90% have durations shorter than 20 min. In order to obtain a tremor location, we applied the waveform envelope cross correlation and clustering (WECC) location scheme from *Wech and Creager* [2008] to locate known tremor bursts regardless of clustering analysis. Using a local 1-D *S* wave velocity model [*Wu et al.*, 2007], we perform a 3-D grid search (horizontal and vertical grid size as 0.1° and 2 km) with the same weighting scheme in WECC method to

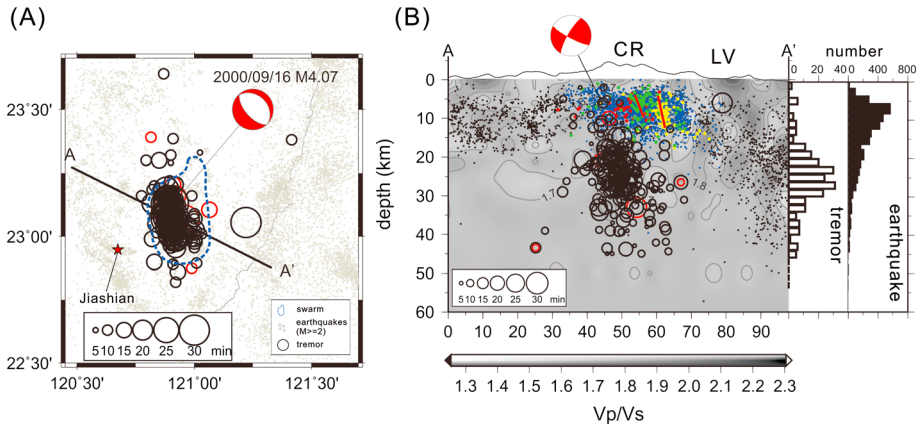

Figure 2. (a) Spatial distribution of ambient tremor events in map view. Open circles indicate location of individual tremor event, and size is scaled with duration from 5 to 30 min. Tremor events have location uncertainties larger than 7 km in vertical and 6 km in horizontal are indicated by red open circles. Blue dashed line circles indicate the locations of earthquake swarms (blue dots in Figure 2b). Red star indicates hypocenter of *M*6.42 Jiashian earthquake. A lower hemisphere projection focal mechanism of local *M*4.07 earthquake is shown in Figure 2a, and lateral hemisphere projection focal mechanism of the same earthquake is also shown in Figure 2b. (b) Cross section along A-A' in Figure 2a. Blue dots indicate earthquake swarms. Red, green, and yellow dots indicate swarm sequences in 2008 and 2010, and red solid lines denote likely fault planes. Open and solid black horizontal bars show number of tremors and earthquakes at different depth. CR and LV denote Central Range and Longitudinal Valley, respectively. Background color shows *Vp/Vs* ratio [*Wu et al.*, 2007]. Gray and black dots shown in Figures 2a and 2b indicate $M \geq 2$ earthquakes, respectively.

obtain an optimized source location. As shown by open circles in Figure 2, most of the detected ambient tremors are confined in a 50×50 km^2 area in southern Central Range with cloud-like structure. Sixty eight percent of the 231 events occurred at a depth range of 17–34 km, below where the seismicity is concentrated (gray and colored dots in Figure 2b).

Applying bootstrap technique, the average location uncertainties are 1 km and 2 km with 95% of the data confined in a range of 7 km and 6 km for the horizontal and vertical components, respectively (Figure S3 in the supporting information). The much greater uncertainties are likely due to smaller number of stations for clear tremor detection (red circle in Figure 2). The location uncertainty is further examined using 63 $M \geq 3.0$ ordinary earthquakes by comparing the earthquake location determined from WECC and the ones from relocated earthquake catalog using 3-D tomography [*Wu et al.*, 2008]. The WECC determined location shows average horizontal and vertical uncertainties of 0.6 and 8.6 km, respectively, whereas their location difference with relocated earthquake catalog are 3.5 km and 6.7 km. This suggests that the WECC location method is comparable to earthquake location uncertainties in this area.

2. Spatial and Temporal Distribution of Ambient Tremors

We investigate the relationship between earthquakes and tremors by comparing the temporal distribution of the detected ambient tremors with background seismicity from January 2008 to December 2011. The number of tremors in each 40 days (vertical gray bar in Figure 3a) is largest at the time of the local 4 March 2010 *M*6.4 Jiashian earthquake (see Figure 1 for the location), where an acceleration pattern lasts for more than 5 months. The cumulative duration of tremors (warm color lines in Figure 3a) appears to change significantly on September 2008, December 2009, March 2010, and January 2011, reflecting changes in the number of tremors per 40 days and suggesting that the study period can be divided into five segments, labeled I to VI. Comparing the number of events in each segment and the shape of a cumulative duration, we found that segments I, III, and VI show a higher rate of tremors at 2.63, 3.62, and 2.81 min/d. Background seismicity shows a similar variation in activity although the highs and lows are more subdued and an increase in tremor in 2011 is nearly undetectable in the activity of the background seismicity. Seismicity in the area of the tremor however occurs in swarms that are highly clustered in space and time without a main shock of sufficient magnitude (red, green, and yellow dots for swarm sequences in Figure 2). These swarms, which are composed of normal faulting (Figure S4 in the supporting information) *M*0.7–*M*3.9 earthquakes during the study period of 2008–2011, occur above the tremor events at <20 km depth and delineate a subvertical

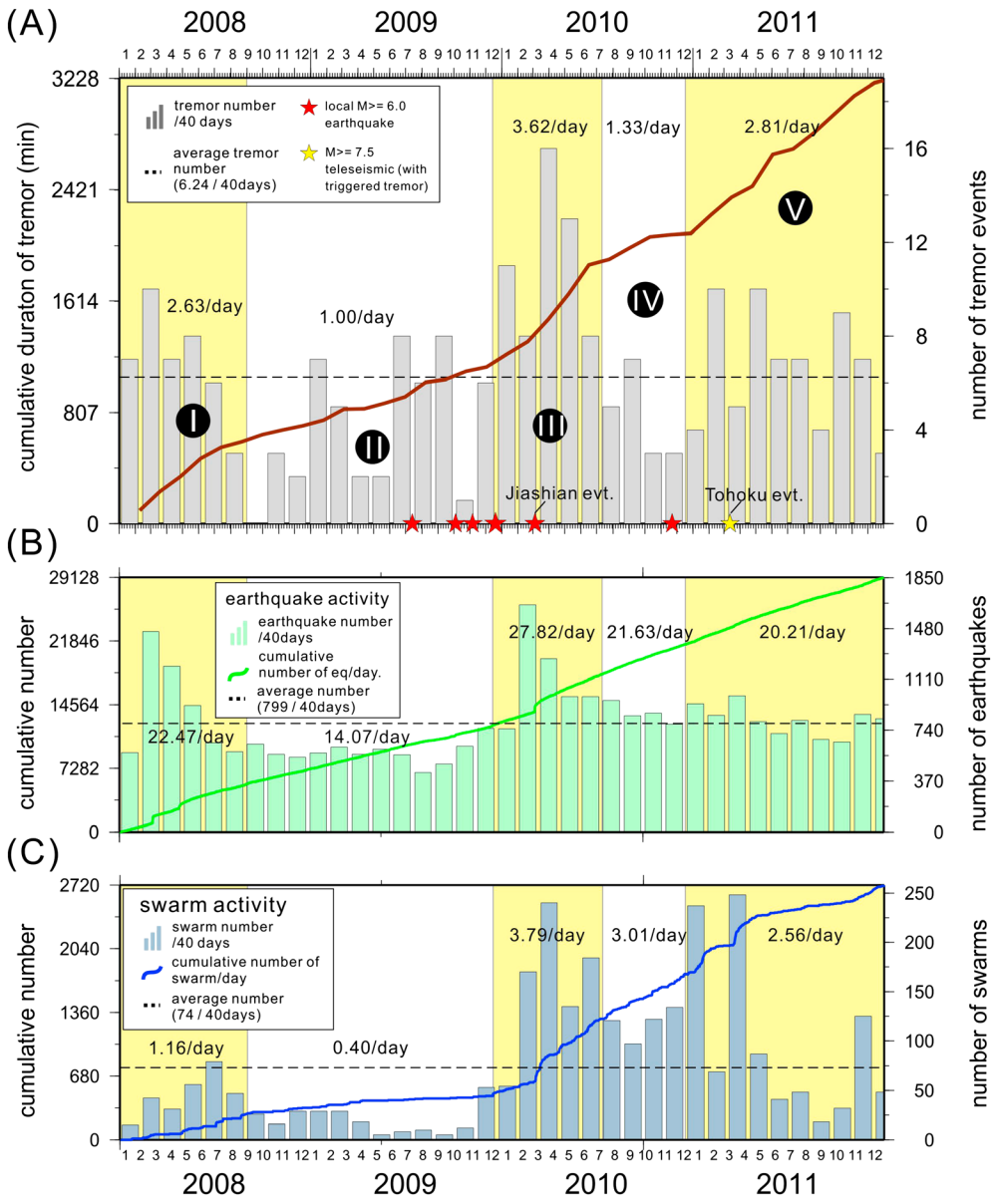

Figure 3. (a) Time distribution of tremor activity from 2008 to 2011. Vertical bar indicates the number of tremor events per 40 days, whereas warm-color lines indicate the cumulative duration of tremor per 40 days. Red stars denote the time of $M \geq 6.0$ earthquakes in Taiwan (locations show in red stars in Figure 1). Yellow star denotes the teleseimsic event on 11 March 2010 (M9.0 Tohoku earthquake). (b) Time distribution of background seismicity from 2008 to 2011. Their locations are indicated by gray and black dots in Figures 2a and 2b, respectively. Vertical bar indicates the number of $M \geq 2$ earthquakes, whereas green line indicates the cumulative number of earthquakes. (c) Time distribution of earthquake swarms from 2008 to 2011(blue dots in Figure 2b). Blue line indicates the cumulative number of earthquake swarms. Horizontal dashed lines from Figures 3a to 3c indicate the average number of tremor, $M \geq 2$ earthquakes, and earthquake swarms, respectively.

planar structure. We find that their activity correlates temporally with tremor as both the tremor and swarm activities are elevated in segments I, III, and VI (Figure 3c).

3. Triggering of Tremors by Static Stress Change Computation

To understand the interaction between tremors and swarms, we consider two hypotheses: (1) the tremors were "triggered" by seismic activity on relatively larger-fault zones close to the field area or (2) the tremors and swarms were triggered "in situ" by local changes in stress and fluid pressure. A combination of these hypotheses is also considered. To study the possible causal relationship between tremor, the Jiashian

earthquake, and the overlying earthquake swarms, we compute the static Coulomb stress changes resulting from both a normal faulting swarm event and the local *M*6.4 Jiashian event on two possible fault planes at the depth of 15–20 km: (1) a thrust fault plane aligned along a décollement suggested by wedge model [*Carena et al*., 2002] and (2) a vertically oriented normal fault plane similar to swarm focal mechanism. Note that the focal mechanism of bigger swarm events shown in Figure S3 in the supporting information is not consistent with the ~90° dip angle revealed from seismicity alignment shown in Figure 2. We explain this as the vertical distribution of hypocenters with normal faulting mechanism reflecting a wide enough vertical zone that contains several parallel or mesh-type normal faulting fractures. In the stress computation, however, we simplify the situation by considering one fault plane instead of multiple fractures. Fault parameters used in the stress change computation are detailed in the supporting information. In this study, an assumption of tremor accompanying with slow slip is made to determine seismic moment of successive tremor using equation (S3) in the supporting information.

The resulting models show that static stress transfer induced by the 4 March 2010 M_w6.4 Jiashian earthquake reveals a ~10 kPa stress change along both the décollement and ~2.5 kPa along a vertical normal faulting structure (Figure S5 in the supporting information). This suggests that the coseismic slip induced Coulomb stress change from the Jiashian earthquake can explain tremors at greater depth. However, there is not a clear correlation between increases in tremor activity (e.g., segments I and V in Figure 3a) and other major earthquakes (red stars in Figure 3a). It is therefore necessary to examine the triggering relationship between tremor and earthquake swarms. We next apply two tremor models (thrust décollement and normal fault) on stress computation. As shown in Figure S6 in the supporting information, the normal fault slip equivalent to M_w3.9 in the earthquake swarm regions transfer smaller positive stress increase of 0.01 kPa near the normal faulting tremor source region, whereas on the thrust décollement, the stress change is negative (−0.01 kPa). When tremor is regarded as a source with equivalent magnitude of M_w4.5, the stress change is calculated to be positive for both source models (0.1 kPa for décollement and normal fault). This result suggests that in addition to the coseismic slip induced Coulomb stress change from the Jiashian earthquake, the small earthquake swarms are also possible to have triggering relationships with the tremor activity at greater depth. Coulomb stress changes on both have triggering scenarios (swarm triggers tremor or tremor triggers swarm) however only occurs when normal faulting of tremor are applied (Figure S6b in the supporting information). If we use thrust faulting as the swarm model, the positive Coulomb stress changes however is gone, suggesting the importance of extensional environment on the triggering relationship.

It is worth noting that the stress changes on the order of 0.1–0.01 kPa from the ~*M*4 events are smaller than tide-induced stress triggering ($<$1 kPa) that will happen if faults are critically stressed [*Rubinstein et al*., 2007]. The triggering relationship could be possible when resistance of faults is reduced by an increase in pore fluid pressures, or both earthquake swarm and tremor activities are driven by some underlying mechanisms such as slow slip and aseismic deformation transients. It is possible that earthquake swarms at shallow depth play a role in elevated tremor activity at deeper levels through a common physical process such as fluid advection or underlying aseismic slip. Under such condition, the static stress triggering may play a secondary role.

4. Possible Generation Mechanism of Tremors in Taiwan

Nonvolcanic tremor has been identified in different tectonic environments. In subduction zones, tremor is thought to be associated with very low effective stress [e.g., *Liu and Rice*, 2005] during shear failure on the plate interface [e.g., *Shelly et al*., 2007] or, alternatively, associated with mineral dehydration under proper temperature and pressure condition [e.g., *Yoshioka et al*., 2008]. In contrast, in transform fault regions, tremor generation is interpreted to be associated to fluid migration and fault weakening [*Becken et al*., 2011]. Unlike subduction zones and transform faults, where the ambient tremors are concentrated near a known fault plane, the tremors observed in Taiwan occur in a place where no volcano or active faults have been identified. The temporal and spatial correlation between deeper tremor and shallow earthquake swarm events suggests a common driving force. The weaker correlation with background seismicity also suggests that background stress changes may play a role (Figure 3b). In Taiwan, the tremors are confined to a small area of 50×50 km^2 under the southern flank of Central Range, coincident with a region characterized by high-heat flow (3.2 W/m^2), a high geothermal gradient (60.6°C/km) [*Chi and Reed*, 2008], and a low *Q* value [*Lee et al*., 2010; *Wang et al*., 2010], suggesting a geothermal anomaly (Figure 4a). Furthermore, the low resistivity (30 Ωm) determined by

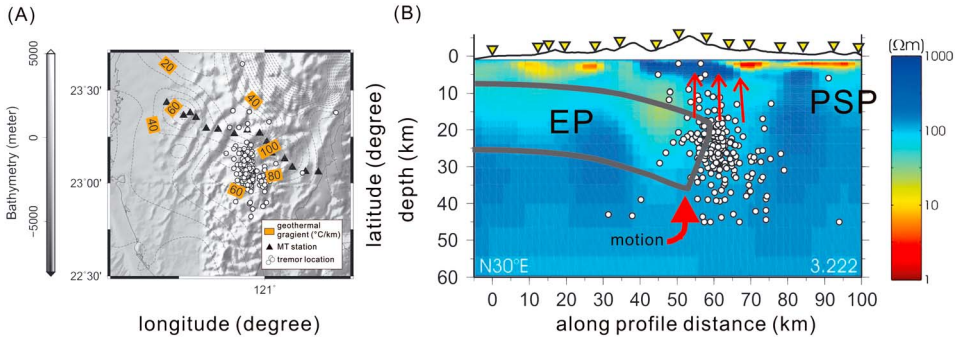

Figure 4. (a) The spatial correlation of tremor location (white circles) and geothermal gradient (contour) by *Chi and Reed* [2008]. (b) Resistivity features by *Bertrand et al.* [2012] along magnetotelluric (MT) profile indicated by MT stations (aligned black triangles) in Figure 4a. The MT network has been deployed by Taiwan Integrated Geodynamic Research project. Location of the Eurasian Plate indicated by gray open rectangle. The abbreviation of PSP denotes Philippine Sea Plate.

magnetotelluric data suggests a fluid content of 0.4–1.4% in the midcrust [*Bertrand et al.*, 2012; *Chiang et al.*, 2010]. Low *Vp* velocities in this area (Figure S7 in the supporting information) are consistent with this interpretation. The normal faulting mechanism of the earthquake swarms located in the shallow crust also imply an extensional environment, and the combination of extensional and rapid uplift may be instrumental in facilitating fluid release from the deeper crust. In other words, individual geophysical studies suggest the existence of fluids in an extensional environment, while seismicity in the same area suggests a connection between deeper tremors and shallow earthquake swarms. As a region that has enough subduction to produce metamorphic fluids [*Hacker et al.*, 2003; *Saffer and Tobin*, 2011] and enough extension to accelerate their release, we propose that this fluid-rock interaction plays an important role in generating the different seismic signals.

5. Conclusion

Under the mountain belt of Taiwan where the rapid exhumation and uplift is taking place, two types of seismic activity typically found in volcanic region occur closely in space. Applying an empirical detection scheme to continuous data from 2008 to 2011, we discovered tremors in a nonvolcanic, collisional tectonic setting; that is the southern Central Range of Taiwan. We locate these tremors below earthquake swarms that occur with normal faulting mechanisms on a subvertical plane $<$20 km deep. We found a significant change in tremor activity at September 2008, December 2009, March 2010, and January 2011, correlating in part, with a local *M*6.4 earthquake and with the overlying earthquake swarms at shallower depth. The greatest acceleration in tremor activity on March 2011 can be explained by the *M*6.4 Jiashian earthquake as the induced Coulomb stress change is positive as 10 kPa for thrust fault plane aligned along the décollement and 2.5 kPa for normal fault plane similar to swarm focal mechanism. The synchronized occurrence of tremor however can also be explained by mutual triggering with earthquake swarm. Normal faulting earthquake swarms that produce a positive stress change in the normal faulting tremors (0.01 kPa for swarm source and 0.1 kPa for tremor source) however is a more likely explanation for tremor acceleration. Unlike the growing evidence that suggests tremor and/or slow slip may lead to large earthquakes, here we find that small to moderate swarm activity in the shallow crust correlates with the occurrence of tremor at greater depth. In addition, the temporal and spatial correlation between deeper tremor and shallow earthquake swarms imply a common generation mechanism. These two seismic activities are confined in a small area that correlates with anomalously high attenuation, the boundary between high and low resistivity and a high thermal anomaly. In addition, the area coincides with a zone now experiencing extension and rapid uplift. This suggests the involvement of metamorphic dehydration and fluid-pressure processes as critical drivers in generating the tremors and swarms within the orogen.

Acknowledgments

We are grateful to Zhigang Peng, Kevin Chao, Robert Nadeau, Roland Bürgmann, Wen-Tzong Liang and Chin-Wu Chen for helpful discussions. We thank the Editor, two anonymous reviewers, and David R. Shelly at USGS for their valuable comments on this manuscript. The seismic data used in this study is provided by Central Weather Bureau Seismic Network (CWBSN) in Taiwan and Broadband Array in Taiwan for Seismology (BATS). This work was supported by Taiwan NSC grant NSC 101-2628-M-003 -001 -MY2.

The Editor thanks two anonymous reviewers for their assistance in evaluating this paper.

References

Aguiar, A. C., T. I. Melbourne, and C. W. Scrivner (2009), Moment release rate of Cascadia tremor constrained by GPS, *J. Geophys. Res.*, *114*, B00A05, doi:10.1029/2008JB005909.

Becken, M., O. Ritter, P. A. Bedrosian, and U. Weckmann (2011), Correlation between deep fluids, tremor and creep along the central San Andreas fault, *Nature*, *480*, 87–90, doi:10.1038/nature10609.

Bertrand, E. A., M. J. Unsworth, C.-W. Chiang, C.-S. Chen, C.-C. Chen, F. T. Wu, E. Türkoğlu, H.-L. Hsu, and G. J. Hill (2012), Magnetotelluric imaging beneath the Taiwan orogen: An arc-continent collision, *J. Geophys. Res.*, *117*, B01402, doi:10.1029/2011JB008688.

Biq, C. (1973), Kinematic pattern of Taiwan as an example of actual continent-arc collision, Rep. Semin. Seismol., US-ROC Coop. Sci. Program (25), 149-166.

Bowin, C., R. S. Lu, C. S. Lee, and H. Schouten (1978), Plate convergence and accretion in Taiwan-Luzon region, *Am. Assoc. Pet. Geol. Bull.*, *62*, 1645–1672.

Carena, S., J. Suppe, and H. Kao (2002), Active detachment of Taiwan illuminated by small earthquakes and its control of first-order topography, *Geology*, *30*(10), 935–938.

Chao, K., Z. Peng, C. Wu, C.-C. Tang, and C.-H. Lin (2012), Remote triggering of non-volcanic tremor around Taiwan, *Geophys. J. Int.*, *188*(1), 301–324, doi:10.1111/j.1365-246X.2011.05261.x.

Chi, W. C., and D. L. Reed (2008), Evolution of shallow, crustal thermal structure from subduction to collision: An example from Taiwan, *Geol. Soc. Am. Bull.*, *120*, 679–690, doi:10.1130/B26210.1.

Chiang, C. W., C. C. Chen, M. J. Unsworth, E. A. Bertrand, C. S. Chen, T. D. Kieu, and H. L. Hsu (2010), The deep electrical structure of southern Taiwan and its tectonic implications, *Terr. Atmos. Ocean. Sci.*, *21*(6), 879–895, doi:10.3319/TAO.2010.02.25.01(T).

Ching, K. E., R. J. Rau, K. M. Johnson, J. C. Lee, and J. C. Hu (2011), Present-day kinematics of active mountain building in Taiwan from GPS observations during 1995–2005, *J. Geophys. Res.*, *116*, B09405, doi:10.1029/2010JB008058.

Davis, D., J. Suppe, and F. A. Dahlen (1983), Mechanics of fold-and-thrust belts and accretionary wedges, *J. Geophys. Res.*, *88*(B2), 1153–1172.

Hacker, B. R., S. M. Peacock, G. A. Abers, and S. D. Holloway (2003), Subduction factory 2. Are intermediate-depth earthquakes in subducting slabs linked to metamorphic dehydration reactions?, *J. Geophys. Res.*, *108*(B1), 2030, doi:10.1029/2001JB001129.

Ho, C. S. (1986), A synthesis of the geologic evolution of Taiwan, *Tectonophysics*, *125*(1–3), 1–16.

Hsu, Y. J., L. Rivera, Y. M. Wu, C. H. Chang, and H. Kanamori (2010), Spatial heterogeneity of tectonic stress and friction in the crust: New evidence from earthquake focal mechanisms in Taiwan, *Geophys. J. Int.*, *182*(1), 329–342.

Ide, S., G. C. Beroza, D. R. Shelly, and T. Uchide (2007), A scaling law for slow earthquakes, *Nature*, *447*, 76–79, doi:10.1038/nature05780.

Lee, C. P., N. Hirata, B. S. Huang, W. G. Huang, and Y. B. Tsai (2010), Evidence of a highly attenuative aseismic zone in the active collision orogen of Taiwan, *Tectonophysics*, *489*(1-4), 128–138.

Liu, Y., and J. R. Rice (2005), Aseismic slip transients emerge spontaneously in three-dimensional rate and state modeling of subduction earthquake sequences, *J. Geophys. Res.*, *110*, B08307, doi:10.1029/2004JB003424.

Peng, Z., and K. Chao (2008), Non-volcanic tremor beneath the Central Range in Taiwan triggered by the 2001 Mw 7.8 Kunlun earthquake, *Geophys. J. Int.*, *175*(2), 825–829, doi:10.1111/j.1365-246X.2008.03886.x.

Rubinstein, J. L., J. E. Vidale, J. Gomberg, P. Bodin, K. C. Creager, and S. D. Malone (2007), Non-volcanic tremor driven by large transient shear stresses, *Nature*, *448*, 579–582, doi:10.1038/nature060.

Saffer, D. M., and H. J. Tobin (2011), Hydrogeology and mechanics of subduction zone forearcs: Fluid flow and pore pressure, *Annu. Rev. Earth Planet. Sci.*, *39*(1), 157–186, doi:10.1146/annurev-earth-040610-133408.

Seno, T., S. Stein, and A. E. Gripp (1993), A model for the motion of the Philippine Sea Plate consistent with NUVEL-1 and geological data, *J. Geophys. Res.*, *98*(B10), 17,941–17,948, doi:10.1029/93JB00782.

Shelly, D. R., G. C. Beroza, S. Ide, and S. Nakamula (2006), Low-frequency earthquakes in Shikoku, Japan, and their relationship to episodic tremor and slip, *Nature*, *442*(7099), 188–191, doi:10.1038/nature04931.

Shelly, D. R., G. C. Beroza, and S. Ide (2007), Non-volcanic tremor and low-frequency earthquake swarms, *Nature*, *446*(7133), 305–307, doi:10.1038/nature05666.

Suppe, J. (1981), Mechanics of mountain building and metamorphism in Taiwan, *Mem. Geol. Soc. China*, *4*, 67–89.

Tang, C.-C., Z. Peng, K. Chao, C.-H. Chen, and C.-H. Lin (2010), Detecting low-frequency earthquakes within non-volcanic tremor in southern Taiwan triggered by the 2005 *Mw*8.6 Nias earthquake, *Geophys. Res. Lett.*, *37*, L16307, doi:10.1029/2010GL043918.

Wang, Y. J., K. F. Ma, F. Mouthereau, and D. Eberhart-Phillips (2010), Three-dimensional Qp- and Qs-tomography beneath Taiwan orogenic belt: Implications for tectonic and thermal structure, *Geophys. J. Int.*, *180*(2), 891–910, doi:10.1111/j.1365-246X.2009.04459.x.

Wech, A. G., and K. C. Creager (2007), Cascadia tremor polarization evidence for plate interface slip, *Geophys. Res. Lett.*, *34*, L22306, doi:10.1029/2007GL031167.

Wech, A. G., and K. C. Creager (2008), Automated detection and location of Cascadia tremor, *Geophys. Res. Lett.*, *35*, L20302, doi:10.1029/2008GL035458.

Wells, D. L., and K. J. Coppersmith (1994), New empirical relationships among magnitude, rupture length, rupture width, rupture area, and surface displacement, *Bull. Seismol. Soc. Am.*, *84*(4), 974–1002.

Willett, S. D., D. Fisher, C. Fuller, Y. En-Chao, and L. Chia-Yu (2003), Erosion rates and orogenic-wedge kinematics in Taiwan inferred from fission-track thermochronometry, *Geology*, *31*(11), 945–948.

Willett, S., C. Beaumont, and P. Fullsack (1993), Mechanical model for the tectonics of doubly vergent compressional orogens, *Geology*, *21*(4), 371–374.

Wu, Y. M., C. H. Chang, L. Zhao, J. B. Shyu, Y. G. Chen, K. Sieh, and J. P. Avouac (2007), Seismic tomography of Taiwan: Improved constraints from a dense network of strong motion stations, *J. Geophys. Res.*, *112*, B08312, doi:10.1029/2007JB004983.

Wu, Y. M., C. H. Chang, L. Zhao, T. L. Teng, and M. Nakamura (2008), A comprehensive relocation of earthquakes in Taiwan from 1991 to 2005, *Bull. Seism. Soc. Am.*, *98*(3), 1471–1481, doi:10.1785/0120070166.

Yamato, P., F. Mouthereau, and E. Burov (2009), Taiwan mountain building: Insights from 2-D thermomechanicalmodelling of a rheologically stratified lithosphere, *Geophys. J. Int.*, *176*(1), 307–326.

Yoshioka, S., M. Toda, and J. Nakajima (2008), Regionality of deep low-frequency earthquakes associated with subduction of the Philippine Sea plate along the Nankai Trough, southwest Japan, *Earth Planet. Sci. Lett.*, *272*(1–2), 189–198.

Yu, S. B., H. Y. Chen, and L. C. Kuo (1997), Velocity field of GPS stations in the Taiwan area, *Tectonophysics*, *274*(1–3), 41–59.